Ecology

Article

Nonlinear effects of temperature on mosquito parasite infection across a large geographic climate gradient

Johannah E. Farner[1*], Kelsey P. Lyberger[2], Lisa I. Couper[3], Mauricio Cruz-Loya[1], Erin A. Mordecai[1]

[1]Department of Biology, Stanford University, Stanford, CA 94305, USA; [2] College of Integrative Sciences and Arts, Arizona State University, Mesa, AZ 85212, USA; [3] Division of Environmental Health Sciences, University of California, Berkeley, Berkeley, CA 94720, USA.

*Corresponding author: jfarner@stanford.edu

Data and code for this submission are provided on

Dryad: http://datadryad.org/stash/share/CfZkk4LsJzljetJJnFZMDMrjuciTXMxrkrc95I2J3tA.

Abstract

Temperature drives ectothermic host – parasite interactions, making them particularly sensitive to climatic variation and change. To isolate the role of temperature, lab-based studies are increasingly used to assess and forecast disease risk under current and future climate conditions. However, in the field, the effects of temperature on parasitism may be mediated by other sources of variation, including local adaptation. To address the key knowledge gaps of how temperature influences host – parasite interactions and whether thermal responses measured in controlled experiments capture infection across temperature gradients in nature, we paired an extensive field survey of parasitism—by the ciliate *Lambornella clarki* on its tree hole mosquito host, *Aedes sierrensis*—with laboratory experiments describing parasitism thermal performance curves (TPCs) for six host populations from varying climates. We also investigated the mechanisms underlying the thermal biology of the host – parasite interaction by separately measuring TPCs for infection, host immunity, and parasite growth rates. Along the west coast of North America, across an 1100 km climate gradient spanning 12ºC mean rainy season temperature variation, we found that parasitism peaked at intermediately cold temperatures, and was consistent both between field seasons and with the lab experiment results. The experiments produced no evidence of host intraspecific variation in temperature sensitivity to parasitism. Importantly, parasitism peaked at temperatures below the thermal optimum for free-living *L. clarki* due to the balance of temperature effects on parasite growth and reproduction against the strength of the host melanization immune response. The results suggest that nonlinear responses to temperature drive parasitism in nature, and that simple lab and field studies can accurately capture the thermal biology of multilayered host – parasite interactions.

Introduction

Climate warming is fundamentally important to disease risk because temperature drives many of the constituent biological processes of host – parasite interactions, including host and parasite growth and development, contact rates, and immune functions (Kutz et al. 2005; Labaude et al. 2017; Laughton, O'Connor, and Knell 2017; Franke et al. 2019; Mordecai et al. 2019). Strong relationships between temperature and parasitism are frequently observed in laboratory experiments and captured in thermal performance curves (TPCs) (Gehman, Hall, and Byers 2018; Kirk et al. 2018; Padfield, Castledine, and Buckling 2020), which researchers then use to assess disease risk based on current and forecasted climate and weather conditions (Gehman, Hall, and Byers 2018; Ryan et al. 2019; Aleuy et al. 2023). However, it is unclear whether TPCs measured in controlled laboratory settings fully capture the thermal response of disease in complex natural settings, where other abiotic and biotic factors may modify or outweigh parasitism - temperature relationships (Mordecai et al. 2019; Taylor et al. 2019; Brown et al. 2023).

Parasitism TPCs are typically measured for single laboratory populations, under constant temperatures, in the absence of other stressors, and are infrequently compared to disease burdens along temperature gradients in the field (e.g., Gehman, Hall and Byers, 2018; Mordecai *et al.*, 2019; Padfield, Castledine and Buckling, 2020). Although an increasing number of studies describe thermal responses for multiple populations or genotypes within host-parasite systems (Mazé-Guilmo et al. 2016; Ahrens et al. 2019; Franke et al. 2019; Aleuy et al. 2023; Ragonese et al. 2024), research on statistical or correlative relationships between TPCs for disease transmissibility (e.g., R_0) and natural infection patterns has thus far relied on laboratory measurements from single populations or clones, and field data collated from disparate sources

and/or collected over small geographic areas. To date, this research has focused primarily on mosquito-borne human disease and fungal pathogens of zooplankton (Mordecai et al. 2013; 2017; Shocket et al. 2018; 2020; Tesla et al. 2018; Shah et al. 2019; Kirk et al. 2024). However, TPCs can vary geographically within species due to local adaptation and population structure (Sinclair, Williams, and Terblanche 2012; Gaitán-Espitia et al. 2014; Mazé-Guilmo et al. 2016; Jurriaans and Hoogenboom 2019; Aleuy et al. 2023; Couper et al. 2024), and additional biotic and abiotic environmental variability in field settings may outweigh or modify the temperature dependence of parasitism (e.g., Boots 2000; Seppälä et al. 2008; Hall et al. 2009; Penczykowski et al. 2014; Palmer-Young et al. 2019; Brown et al. 2023). Thus, there is a critical need to address the questions of how temperature affects parasitism in the field, whether lab-based TPC estimates can accurately, and mechanistically, capture these patterns, and whether local adaptation modifies the temperature-dependence of parasitism.

Central to capturing the thermal biology of parasitism is understanding the host and parasite mechanisms that drive the interaction. For example, host life history and defense traits and parasite growth, attack, dispersal, and transmission traits may each respond nonlinearly and distinctly to temperature. The combined effect of these traits determines the overall impact of temperature on parasitism (Paull, LaFonte, and Johnson 2012; Shocket et al. 2018; Mordecai et al. 2019; Sun et al. 2023). Moreover, host and parasite traits may differ across populations due to local adaptation and across environmental conditions (Thomas and Blanford 2003; Sternberg and Thomas 2014). Given that it is not feasible to measure TPCs for every possible combination of host population, parasite population, and environmental context, it is important to establish whether TPCs measured for a single set of populations and conditions can generalize to cover entire species ranges, and which traits capture the essential thermal biology of the interaction.

Here, we address these questions in a highly tractable experimental model system of a mosquito (*Aedes sierrensis*) and its facultative ciliate parasite (*Lambornella clarki*), which occur across a large geographic gradient in western North America.

In this study, we pair field surveys along the entire west coast of the continental United States—spanning the geographic range of the host species—with laboratory experiments describing the temperature dependence of infection and key traits for host populations from different climates across the survey area. Both species are short-lived ectotherms that are directly affected by environmental temperatures, occur commonly across a large geographic climate gradient in discrete tree hole habitats that are naturally replicated across landscapes, and can be reared separately and together in the lab (Washburn and Anderson 1986; Broberg and Bradshaw 1997; Darsie and Ward 2005; Ismail et al. 2023; Lyberger et al. 2024). A 1986 field survey found that infection occurrence increased from southern to northern California (Washburn and Anderson 1986). Our recent work describing temperature effects on different populations of *Ae. sierrensis, L. clarki*, and their interactions indicates that infection has a consistent nonlinear relationship with temperature for both sympatric and allopatric pairs of host and parasite populations collected across climates, despite evidence of local thermal adaptation in free-living *L. clarki* populations (Ismail et al. 2023; Lyberger et al. 2024). This body of work generates the hypothesis that parasitism responds to temperature as a function of the thermal biology of multiple host and parasite traits. However, it is unknown whether the lab-measured temperature impacts on parasitism across different *Ae. sierrensis* host populations are borne out in infection occurrence across the environmentally complex species range.

Methods

Study system

Ae. sierrensis and its facultative ciliate parasite *L. clarki* occur across western North America in seasonally rainwater-filled tree holes, where mosquitoes undergo one reproductive cycle annually in which larvae feed on detritus and microbes (including free-living *L. clarki*) before pupating and emerging as adults, and free-living *L. clarki* ciliates feed on aquatic bacteria (Washburn and Anderson 1986; Darsie and Ward, 2005). In the presence of *Ae. sierrensis* larvae, free-living *L. clarki* irreversibly transform into parasites that attack larval mosquitoes and often kill them after a few weeks (Washburn et al., 1988). Mosquitoes can resist infection through multiple defenses that each likely respond nonlinearly to temperature: melanization (a generalized immune response), molting between larval instars, developing into pupae, and consuming free-living *L. clarki* in the water column (Clark and Brandl 1976; Washburn et al. 1988; Washburn, Anderson, and Mercer 1991; Suwanchaichinda and Paskewitz 1998; Christensen et al. 2005; Murdock et al. 2012; Martin and Hillyer 2024). Beyond the previously documented latitudinal gradient, *L. clarki* presence is not correlated with habitat characteristics such as tree hole size, exposure, height above ground, or tree species (Washburn and Anderson 1986).

Field survey

To document infection patterns over a large geographic temperature gradient and collect materials for lab experiments, we sampled from over 500 water-filled tree hole habitats containing *Ae. sierrensis* larvae spanning 1100 km north to south with a mean November – April rainy season temperature gradient of 2.6ºC to 15.3ºC in California, Oregon, and Washington, USA, during the rainy seasons of 2022 and 2023 (Figure 1) (PRISM Climate Group, 2021). Each

year, we started in the warmest and ended in the coolest locations to track the seasonal timing of *Ae. sierrensis* egg hatching and development (Jordan and Bradshaw 1978; Jordan 1980a; 1980b), collecting larval samples and examining them for infection at 10-40x magnification (Appendix S1). We aimed to sample each tree hole in both years, but had to replace some locations in 2023 due to storm damage (Figure 1).

For each sampling site, we used PRISM climate data to characterize long-term mean temperature and precipitation conditions in the November – April rainy season when mosquito larvae and parasites are active in tree holes, and Rainy and Dry Season (RADS) data to characterize the median wet season duration (Bombardi, Kinter, and Frauenfeld 2019; PRISM Climate Group and Oregon State University 2021; Washburn and Anderson 1986; Luković et al. 2021; Praskievicz and Chang 2009). We also placed iButton temperature loggers (Maxim Integrated, San Jose, CA, USA) in 84 arbitrarily selected tree holes across the survey area from 2022 to 2023 to assess how local temperatures compared to PRISM. Finally, we accessed NOAA climate reports that compared regional temperatures and precipitation in each field season to long-term averages (NOAA National Centers for Environmental Information 2022; 2023). Additional details on the field survey methods are provided in Appendix S1.

Lab experiments

1. Temperature-dependent infection experiment

In September 2022, we measured the effects of temperature on the host – parasite interaction with an experiment that used the F1 offspring of six host populations reared in the lab from larvae collected in the 2022 field survey: two each from warm (14.8 – 15.1ºC rainy season mean temperature; San Juan Capistrano and Trabuco Canyon, CA), intermediate (10.8 – 11.8ºC; Big

157 Sur and Woodside, CA), and cool (5.3 – 6.5ºC; Shaver Lake, CA and Eugene, OR) climates
158 (Figure 1, Appendix S2: Table S1). We exposed each host population to the same allopatric
159 parasite culture isolated from an infected larva collected in Marin County, CA (10.6ºC) (Figure
160 1), so that any variation observed in the temperature dependence of infection would be due to the
161 host population. Mosquito rearing and ciliate culturing occurred at 21.5ºC following Ismail *et al.*
162 (2023), Couper *et al.* (2024), and Lyberger *et al.* (2024).

163 For the experiment, mosquito eggs were hatched and day-old larvae were incubated in groups
164 of five with 7 mL parasite culture diluted to a standardized density of 35 ciliates per 100 uL at six
165 constant temperatures: 7ºC, 11ºC, 14ºC, 18ºC, 23ºC, and 28ºC (N = 6 microcosms per host
166 population per temperature, except for Big Sur, where N = 4 due to lower egg hatching). We
167 monitored the proportions of hosts with infections and parasite melanization spots, and the
168 survival of infected and uninfected hosts, up to the first pupation at each temperature. Because
169 *Ae. sierrensis* development speed is thermally sensitive, we set monitoring frequences that
170 ensured at least four checkpoints spanning the host's four larval instars at each temperature; these
171 ranged from every two days at 28ºC to every seven days at 7ºC and 11ºC (Appendix S2: Table
172 S2).

173 2. *Host and parasite thermal responses in isolation*

174 To compare the thermal performance of mosquito larvae and ciliates to that of parasitism, we
175 incubated mosquito-only and ciliate-only microcosms alongside the infection experiment,
176 following the same design as above. The mosquito-only microcosms were monitored on the
177 same timeline as the infection experiment. For the ciliate-only microcosms, we measured the
178 population growth rate by inoculating wells with culture diluted to 4 cells per 100 uL and then
179 counting the cells per 300 uL daily for four days of positive growth.

To assess the temperature sensitivity of the host melanization process (removing the temperature sensitivity of parasite attack rates), we performed a mechanical melanization assay on fourth instar larvae from one population at 4, 8, 12, 16, 20, 24, and 28ºC (N = 6 wells of 5 mosquitoes per temperature with no ciliates). Additional details are provided in Appendix S1.

Statistical analyses

Field survey

To investigate the nonlinear temperature dependence of parasitism, we tested for a quadratic relationship between temperature and the presence of *L. clarki* infections in the surveyed tree holes using a binomial generalized linear mixed effects model, with mean temperature, mean temperature squared, and year as fixed effects, and tree hole ID as a random effect. The final model did not include precipitation metrics because of strong correlations between temperature and precipitation variables (R^2 = -0.8 for both cumulative precipitation and median wet season duration), and because we expect temperature to more directly affect the host-parasite interaction, as precipitation was sufficient across all sampled locations for tree holes to fill with water and *Ae. sierrensis* to occur. We used the glmer function in the R package "lme4" with scaled and centered environmental variables, and assessed model fit with the R package "DHARMa" (Bates et al. 2003; Hartig 2017). Because interactions between survey year and the temperature variables were not significant, we estimated the overall mean temperature where infection was most likely to occur with a model that did not include year. We additionally used general linearized models fit individually to the data from each survey year to describe the temperatures where infection occurrence peaked within each field season. To evaluate the relationship between within-tree hole habitat temperatures logged by iButtons and the PRISM air temperature dataset used in the model, we tested for correlations and calculated the mean

differences between daily mean temperature time series recorded by iButtons and extracted from PRISM. Because there were only two field seasons, the NOAA annual climate reports for each field season were not included in statistical analyses, but used only to qualitatively compare the two years.

Lab experiments

To quantify the thermal sensitivity of the host – parasite interaction measured from the laboratory experiment, we used a Bayesian approach to fit TPCs for the proportion of infected hosts, the proportion of hosts with melanization spots, and the proportion of hosts killed by infections. The total number of infections observed in each microcosm over the course of the experiment depended on both initial parasite attack success and subsequent rounds of parasite transmission following infected host deaths that released new parasites as killed mosquitoes decomposed. We fit separate TPCs for both initial infection for the period up to the first deaths of infected hosts at each temperature, when all observed infections resulted from the first round of host – parasite interactions (covering checkpoints 1-3, approximately corresponding to larval instars 1-3), and total infection rates over the entire experiment (including all host-parasite interaction cycles for all four larval instars); we used the same procedure to fit initial and total TPCs for the proportions of hosts melanizing attacking parasites. We additionally fit TPCs for free-living *L. clarki* population growth rate and for the host melanization immune response induced by mechanical penetration of the cuticle. We planned to fit TPCs for host survival in the absence of parasitism, but >99% of larvae incubated without parasites survived across all temperatures. Because initial parasite success is likely to determine whether there is a non-zero infection probability over the rest of the season (Washburn, Anderson, and Mercer 1991), this is

the laboratory-based TPC that we expect to most closely align with the field-observed response of infection occurrence to temperature.

Unimodal traits were fit with a flexTPC functional form (Equation 1) which can describe unimodal TPCs of any skewness (Cruz-Loya, Mordecai and Savage, *preprint*). Using this flexible function to fit TPCs of different shapes across our traits of interest allowed for ease of comparison of thermal responses among traits and populations.

$$r(T) = \begin{cases} r_{max}\left[\left(\frac{T - T_{min}}{\alpha}\right)^{\alpha}\left(\frac{T_{max} - T}{1-\alpha}\right)^{1-\alpha}\left(\frac{1}{T_{max} - T_{min}}\right)\right]^{\frac{\alpha(1-\alpha)}{\beta^2}} & T_{min} < T < T_{max} \\ 0 & \text{otherwise} \end{cases} \quad (1)$$

In this equation, T_{min} and T_{max} correspond to the minimum and maximum temperature, respectively, r_{max} to the maximum trait value, and α and β are parameters that determine the curve skewness and rate of decrease from the maximum trait value (Appendix S1). Host melanization increased monotonically with temperature, and was fit to a 4-parameter shifted logistic model (Equation 2, see Appendix S1 for derivation).

$$m(T) = \begin{cases} \frac{1}{\left[1 + (2^{1/s} - 1)\left(\frac{T_{50} - T_{min}}{T - T_{min}}\right)^{a}\right]^{s}} & T > T_{min} \\ 0 & \text{otherwise} \end{cases} \quad (2)$$

where T_{min} is the minimum temperature, T_{50} is the temperature at which 50% of the population is melanized, and a and s are constants that allow for different rates of change of melanization near T_{50} and for the response to be asymmetric, which was necessary to fit the data.

We used a binomial likelihood for all traits that were measured as proportions. For the free-living parasite population growth rate TPC, we used a Gamma likelihood with population growth rates obtained from the raw time-course data with the R package “growthrates” (Petzoldt 2022).

Optimal temperatures were calculated analytically using the posterior samples of the model parameters (Appendix S1).

To assess population variation in lab-measured thermal performance among host populations and the responses measured in the infection experiment, we compared 95% credible intervals for the thermal optimum (T_{opt}), maximum (T_{max}), and minimum (T_{min}) and interpreted non-overlapping intervals as evidence of biologically significant variation. We additionally compared the magnitudes of the 95% credible intervals over TPC plots for each population. Since the credible intervals for T_{opt}, T_{min}, and T_{max} overlapped for all populations for all measured traits, we combined the data to generate species-representative TPCs, which we used for our main analyses and interpretations. Finally, we compared the parasitism TPC to the host and parasite trait TPCs measured in isolation.

We used R version 4.2.1 for all statistical analyses and for figure generation. See Appendix S1 for additional details and R packages used.

Results

Does infection occurrence vary with climate across the species range?

Infection occurrence followed a hump-shaped pattern along the surveyed temperature gradient, peaking at 9.4ºC mean rainy season temperature (Figure 2). Mean temperature^2 and year were significant predictors of *L. clarki* infection presence (Table 1). Quadratic models fit individually for infection occurrence in each year peaked at 10.0ºC in 2022 and 9.2ºC in 2023, but the interactions between year and both temperature variables were not statistically significant (Table 1). Geographically, infections were common in northern California and southern Oregon

266 and rarer at the warm and cold ends of the surveyed temperature gradient in southern California
267 and northern Washington, respectively (Figure 1).
268 Of the two sampling years, 2023 was cooler and wetter and had a higher percentage of
269 infected tree holes (29.7%, N = 431) compared to 2022 (12.5%, N = 320) (Figure 2) (NOAA
270 National Centers for Environmental Information 2022; 2023). Tree hole habitat temperatures
271 logged by iButtons (N = 32 successfully retrieved) did not systematically differ from PRISM air
272 temperature estimates (mean temperature difference = 1.3ºC, SD = 2.6ºC; R^2 mean = 0.94, SD =
273 0.03) (Appendix S2: Figure S1). Additional details are provided in Appendix S2.
274
275 *Does the thermal response of the host – parasite interaction depend on the host population?*
276 We found similar thermal optima, minima and maxima across the six host populations in the
277 infection experiment within each of the three measured interaction outcomes of infection,
278 melanization of parasites, and mortality (Figure 3; Appendix S2: Figures S2-S11; Tables S3-S7).
279 Although the mean estimated T_{opt}, T_{min}, and T_{max} varied slightly among populations for each
280 trait, all 95% credible intervals across populations for each outcome x parameter combination
281 overlapped. Therefore, we combined the data for all host populations to estimate broadly
282 representative TPCs for the host – parasite interaction, with reduced uncertainty compared to the
283 population-specific TPCs (Figure 4; Appendix S2: Figure S12; Table S9). The only trait in which
284 we observed clear intraspecific variation was in mortality around 10ºC, which was higher in one
285 intermediate climate population (Big Sur (BIG)) compared to the other (Woodside (JR)) and to
286 one cold climate population (Eugene (EUG)) (Figure S13).
287

How do different components of the host – parasite interaction relate to the overall thermal sensitivity of parasitism?

Although free-living parasite population growth was maximized at warm temperatures, infection and parasite-induced mortality peaked at significantly colder temperatures, corresponding to conditions that suppressed host defense mechanisms, namely the melanization immune response and larval development speed (Figure 4). Specifically, the initial infection rate peaked at 10ºC (95% CI: 8.7 ºC, 11.3 ºC), and the total infection rate peaked at 8.4ºC (95% CI: 6.8 ºC, 9.4 ºC), much lower temperatures than the 19.5ºC (95% CI: 18.9 ºC, 20.2 ºC) optimum for free-living parasite population growth (Figure 4A; Appendix S2: Figure S12; Tables S8-9). The mechanically assayed host melanization immune response increased with temperature up to 20ºC, where it plateaued (Figure 4A; Appendix S2: Table S10). At warmer temperatures, attacking parasites faced not only a stronger host immune response, but also shorter time windows in which to infect hosts without being shed with the cuticle during larval molting and pupation or eaten by later larval instars. The time to the first observed pupation shortened as the temperature increased, occurring after 9 days at 28ºC compared to 57 days at 7ºC (Figure 4B), consistent with previously measured *Ae. sierrensis* larval development rate TPCs that peaked at 27.7ºC (Couper *et al.*, 2024). Consequently, quick pupation interrupted upward trajectories of infection and mortality at intermediate temperatures, contributing to the decline in parasitism above 11ºC, and to the lower T_{opt} of total compared to initial infection.

Discussion

In this study, we used complementary field observations and lab experiments to understand how temperature affects a host-parasite interaction across a large, climatically variable species

range. We found that infection peaked at sites with intermediate temperatures (9.4ºC) in the field and in a colder, wetter year, aligning with the unimodal temperature-dependence of infection measured in the lab, which peaked at 10ºC. This reflects the interacting thermal biology of multiple mosquito and ciliate traits, which together led to an optimal temperature for parasitism (8-10ºC for total versus initial infection) that was colder than the optimal temperature for free-living parasite performance (19.5ºC). Infection rates of mosquito populations from different climates had similar thermal responses in the lab, and a single TPC described the infection process across the entire surveyed area. These findings suggest that TPCs measured under simplified lab conditions can capture both patterns of parasitism across large geographic temperature gradients in complex natural settings and the underlying thermal biology mechanisms.

Lab experiments capture nonlinear parasitism thermal responses in the field

The results add to evidence that temperature nonlinearly affects parasitism not only in the lab, but also in nature, making laboratory and field studies that are designed to capture nonlinear temperature effects valuable tools for understanding disease risk (Dudney et al. 2021; Kirk et al. 2024; Shocket, Ryan, and Mordecai 2018). However, despite the similarities between the field observations and the lab-measured parasitism TPC, we cannot rule out the influence of other factors. For example, the colder survey year with higher infection prevalence was also wetter, suggesting that precipitation patterns that determined when and for how long tree holes were water-filled may have also affected the potential for parasitism to occur. These limitations should be addressed with field experiments that manipulate temperatures in natural tree holes at

333 different latitudes or elevations; lab experiments that incorporate additional environmental
334 complexity; and long term repeated yearly sampling of the same tree holes.
335
336 *Intraspecific variation*
337 Very few studies investigate the impact of local thermal adaptation on species distributions
338 and host – parasite interactions, a gap often noted in the literature (Sternberg and Thomas 2014;
339 Urban et al. 2016; Couper et al. 2021; Aleuy et al. 2023). In addressing this gap, we did not find
340 evidence of local temperature adaptation affecting infection patterns across temperatures in the
341 lab or the field, consistent with our previous work on sympatric and allopatric host – parasite
342 interactions over a narrower temperature range, and despite our previous findings that both *Ae.*
343 *sierrensis* pupal development and *L. clarki* free-living population growth rates are locally
344 adapted to temperature (Lyberger et al. 2024; Couper et al. 2024; Ismail et al. 2023). However,
345 this is one of the only ectothermic host – parasite systems for which interaction thermal
346 sensitivity has been assessed for populations from different climates, along with a stickleback –
347 tapeworm system in which effects of temperature on parasitism were similar among four study
348 populations collected from across a similar geographic temperature gradient (Franke et al. 2019).
349 Notably, intraspecific variation in parasitism temperature sensitivity has been shown for levels of
350 biological organization both above and below the population level that we assessed, for
351 *Batrachochytrium dendrobatitis* infection both among different frog host species, and among
352 salamander host color morphs within a single population (Cohen et al. 2017; Venesky et al.
353 2022). However, if population thermal sensitivities of parasitism are commonly consistent across
354 species ranges, broadly applicable TPCs should be easily attainable for the many host – parasite

systems that are amenable to laboratory studies, and field studies may also be able to capture nonlinear responses of parasitism to temperature.

Mechanisms of parasitism temperature dependence

Our finding that parasitism peaked at temperatures that constrained host development and defense—rather than at the thermal optimum for parasite growth and attack—aligns with theory on the thermal biology of biotic interactions. Thermal asymmetry theory posits that parasitism peaks at temperatures where parasites outperform hosts, which may differ from optimal temperatures for the parasites themselves (Dell, Pawar, and Savage 2014; Cohen et al. 2017). Our study supports the value of approaching this problem as the outcome of multiple interacting host and parasite traits with varying thermal responses (Paull, LaFonte, and Johnson 2012; Marta S. Shocket et al. 2018; Sun et al. 2023).

Conclusions

Overall, our characterization of the temperature – infection relationship of the *Ae. sierrensis* host – *L. clarki* parasite interaction across settings demonstrates how controlled lab experiments can be paired with large-scale field observations to understand the complex thermal biology of parasitism. Climate warming is expected to cause geographic contractions, expansions, and shifts in host thermal refuges from disease (Altizer et al. 2013; Gsell et al. 2023). Our results suggest that parasitism burdens on *Ae. sierrensis* may decline at southern latitudes and low elevations as thermally suitable conditions for parasitism shift northwards and upwards into areas where cold conditions currently limit *L. clarki* infections. Whether the distribution of parasitism ultimately tracks climate warming will depend on multiple factors, including parasite dispersal and the

effects of other environmental changes in conjunction with increasing mean temperatures, such as increasingly extreme precipitation patterns (Swain et al. 2018). Understanding how temperature affects parasitism in inherently complex and variable natural systems remains a pressing problem with broad implications for current and future disease risk management. Simple pairings of field surveys and lab experiments can offer straightforward means for approaching this challenge.

Acknowledgments

Otto Seppälä, Jan Washburn, Nona Chiariello, and Angie Nakano played critical roles in establishing the study system. Our field sampling and mosquito rearing efforts were made possible by assistance from staff at vector control agencies for the California counties of San Mateo, Santa Clara, Marin-Sonoma, Solano, Alameda, Shasta, Placer, Santa Barbara, and Riverside; Jasper Ridge Biological Preserve ‘Ootchamin ‘Ooyakma; the UC Reserves at Emerson Oaks, Dawson Los Monos Canyon, and Hopland; and Andrew Rivera of Clarke Pest Control. Mordecai lab members helped with setting up the infection experiment. JEF was funded by the Bing-Mooney Fellowship and the ARCS Foundation. EAM and MCL were supported by the National Institutes of Health (R35GM133439 and R01AI168097). EAM was supported by the National Science Foundation (DEB-2011147 with Fogarty International Center), the National (R01AI102918), the Stanford Woods Institute for the Environment, the Stanford Center for Innovation in Global Health, and the Stanford Doerr School of Sustainability. KL was funded by the NSF Postdoctoral Research Fellowships in Biology Program under Grant No. 2208947. LIC was funded by the NSF Postdoctoral Research Fellowship in Biology. MCL was supported by a Stanford PRISM Baker Fellowship.

References

Ahrens, Collin W., Richard A. Mazanec, Trudy Paap, Katinka X. Ruthrof, Anthea Challis, Giles Hardy, Margaret Byrne, David T. Tissue, and Paul D. Rymer. 2019. "Adaptive Variation for Growth and Resistance to a Novel Pathogen along Climatic Gradients in a Foundation Tree." *Evolutionary Applications* 12 (6): 1178–90. https://doi.org/10.1111/eva.12796.

Aleuy, O. Alejandro, Stephanie J. Peacock, Péter K. Molnár, Kathreen E. Ruckstuhl, and Susan J. Kutz. 2023. "Local Thermal Adaptation and Local Temperature Regimes Drive the Performance of a Parasitic Helminth under Climate Change: The Case of *Marshallagia marshalli* from Wild Ungulates." *Global Change Biology* 29 (22): 6217–33. https://doi.org/10.1111/gcb.16918.

Altizer, Sonia, Richard S. Ostfeld, Pieter T. J. Johnson, Susan Kutz, and C. Drew Harvell. 2013. "Climate Change and Infectious Diseases: From Evidence to a Predictive Framework." *Science* 341 (6145): 514–19. https://doi.org/10.1126/science.1239401.

Bates, Douglas, Martin Maechler, Ben Bolker, and Steven Walker. 2003. "Lme4: Linear Mixed-Effects Models Using 'Eigen' and S4." https://doi.org/10.32614/CRAN.package.lme4.

Bombardi, Rodrigo J., James L. Kinter, and Oliver W. Frauenfeld. 2019. "A Global Gridded Dataset of the Characteristics of the Rainy And Dry Seasons." *Bulletin of the American Meteorological Society* 100 (7): 1315–28. https://doi.org/10.1175/BAMS-D-18-0177.1.

Boots, M. 2000. "Density-Independent Resource Limitation and the Transmission of an Insect Pathogen." *Oecologia* 124 (2): 172–75. https://doi.org/10.1007/s004420050004.

Broberg, Leonard E., and William E. Bradshaw. 1997. "*Lambornella clarki* (Ciliophora: Tetrahymenidae) Resistance in *Aedes sierrensis* (Diptera: Culicidae): Population

Differentiation in a Quantitative Trait and Allozyme Loci." *Journal of Medical Entomology* 34 (1): 38–45. https://doi.org/10.1093/jmedent/34.1.38.

Brown, Joel J., Mercedes Pascual, Michael C. Wimberly, Leah R. Johnson, and Courtney C. Murdock. 2023. "Humidity – The Overlooked Variable in the Thermal Biology of Mosquito-Borne Disease." *Ecology Letters* 26 (7): 1029–49. https://doi.org/10.1111/ele.14228.

Christensen, Bruce M., Jianyong Li, Cheng-Chen Chen, and Anthony J. Nappi. 2005. "Melanization Immune Responses in Mosquito Vectors." *Trends in Parasitology* 21 (4): 192–99. https://doi.org/10.1016/j.pt.2005.02.007.

Clark, T.B., and D.G. Brandl. 1976. "Observations on the Infection of *Aedes sierrensis* by a Tetrahymenine Ciliate." *Journal of Invertebrate Pathology* 28 (3): 341–49. https://doi.org/10.1016/0022-2011(76)90009-4.

Cohen, Jeremy M., Matthew D. Venesky, Erin L. Sauer, David J. Civitello, Taegan A. McMahon, Elizabeth A. Roznik, and Jason R. Rohr. 2017. "The Thermal Mismatch Hypothesis Explains Host Susceptibility to an Emerging Infectious Disease." Edited by Richard Ostfeld. *Ecology Letters* 20 (2): 184–93. https://doi.org/10.1111/ele.12720.

Couper, Lisa I., Johannah E. Farner, Jamie M. Caldwell, Marissa L. Childs, Mallory J. Harris, Devin G. Kirk, Nicole Nova, et al. 2021. "How Will Mosquitoes Adapt to Climate Warming?" Edited by George H Perry. *eLife* 10 (August):e69630. https://doi.org/10.7554/eLife.69630.

Couper, Lisa I., Johannah E. Farner, Kelsey P. Lyberger, Alexandra S. Lee, and Erin A. Mordecai. 2024. "Mosquito Thermal Tolerance Is Remarkably Constrained across a

Large Climatic Range." *Proceedings of the Royal Society B: Biological Sciences* 291 (2015): 20232457. https://doi.org/10.1098/rspb.2023.2457.

Cruz-Loya, Mauricio, Erin A. Mordecai, and Van M. Savage. 2024. "A Flexible Model for Thermal Performance Curves." *bioRxiv*, January, 2024.08.01.605695. https://doi.org/10.1101/2024.08.01.605695.

Darsie, Richard F., and Ronald A. Ward. 2005. *Identification and Geographical Distribution of the Mosquitoes of North America, North of Mexico*. University Press of Florida.

Dell, Anthony I., Samraat Pawar, and Van M. Savage. 2014. "Temperature Dependence of Trophic Interactions Are Driven by Asymmetry of Species Responses and Foraging Strategy." *Journal of Animal Ecology* 83 (1): 70–84. https://doi.org/10.1111/1365-2656.12081.

Dudney, Joan, Claire E. Willing, Adrian J. Das, Andrew M. Latimer, Jonathan C. B. Nesmith, and John J. Battles. 2021. "Nonlinear Shifts in Infectious Rust Disease Due to Climate Change." *Nature Communications* 12 (1): 5102. https://doi.org/10.1038/s41467-021-25182-6.

Franke, Frederik, Nadja Raifarth, Joachim Kurtz, and Jörn P. Scharsack. 2019. "Consequences of Divergent Temperature Optima in a Host–Parasite System." *Oikos* 128 (6): 869–80. https://doi.org/10.1111/oik.05864.

Gaitán-Espitia, Juan Diego, Leonardo D. Bacigalupe, Tania Opitz, Nelson A. Lagos, Tania Timmermann, and Marco A. Lardies. 2014. "Geographic Variation in Thermal Physiological Performance of the Intertidal Crab *Petrolisthes violaceus* along a Latitudinal Gradient." *Journal of Experimental Biology* 217 (24): 4379–86. https://doi.org/10.1242/jeb.108217.

Gehman, Alyssa-Lois M., Richard J. Hall, and James E. Byers. 2018. "Host and Parasite Thermal Ecology Jointly Determine the Effect of Climate Warming on Epidemic Dynamics." *Proceedings of the National Academy of Sciences* 115 (4): 744–49. https://doi.org/10.1073/pnas.1705067115.

Gsell, Alena S., Arjen Biere, Wietse de Boer, Irene de Bruijn, Götz Eichhorn, Thijs Frenken, Stefan Geisen, et al. 2023. "Environmental Refuges from Disease in Host–Parasite Interactions under Global Change." *Ecology* 104 (4): e4001. https://doi.org/10.1002/ecy.4001.

Hall, Spencer R., Joseph L. Simonis, Roger M. Nisbet, Alan J. Tessier, and Carla E. Cáceres. 2009. "Resource Ecology of Virulence in a Planktonic Host-Parasite System: An Explanation Using Dynamic Energy Budgets." *The American Naturalist* 174 (2): 149–62. https://doi.org/10.1086/600086.

Hartig, Florian. 2017. "Package 'Dharma.'" *R Package*.

Ismail, Sherine, Johannah Farner, Lisa Couper, Erin Mordecai, and Kelsey Lyberger. 2023. "Temperature and Intraspecific Variation Affect Host–Parasite Interactions." *Oecologia*, November. https://doi.org/10.1007/s00442-023-05481-z.

Jordan, R. G., and W. E. Bradshaw. 1978. "Geographic Variation in the Photoperiodic Response of the Western Tree-Hole Mosquito, *Aedes sierrensis*." *Annals of the Entomological Society of America* 71 (4): 487–90. https://doi.org/10.1093/aesa/71.4.487.

Jordan, Robert G. 1980a. "Embryonic Diapause in Three Populations of the Western Tree Hole Mosquito, *Aedes sierrensis*." *Annals of the Entomological Society of America* 73 (4): 357–59. https://doi.org/10.1093/aesa/73.4.357.

———. 1980b. “Geographic Differentiation in the Development *of Aedes sierrensis* (Diptera: Culicidae) in Nature.” *The Canadian Entomologist* 112 (2): 205–10. https://doi.org/10.4039/Ent112205-2.

Jurriaans, S., and M. O. Hoogenboom. 2019. “Thermal Performance of Scleractinian Corals along a Latitudinal Gradient on the Great Barrier Reef.” *Philosophical Transactions of the Royal Society B: Biological Sciences* 374 (1778): 20180546. https://doi.org/10.1098/rstb.2018.0546.

Kirk, Devin, Natalie Jones, Stephanie Peacock, Jessica Phillips, Péter K. Molnár, Martin Krkošek, and Pepijn Luijckx. 2018. “Empirical Evidence That Metabolic Theory Describes the Temperature Dependency of Within-Host Parasite Dynamics.” *PLOS Biology* 16 (2): e2004608. https://doi.org/10.1371/journal.pbio.2004608.

Kirk, Devin, Samantha Straus, Marissa L. Childs, Mallory Harris, Lisa Couper, T. Jonathan Davies, Coreen Forbes, et al. 2024. “Temperature Impacts on Dengue Incidence Are Nonlinear and Mediated by Climatic and Socioeconomic Factors: A Meta-Analysis.” *PLOS Climate* 3 (3): e0000152. https://doi.org/10.1371/journal.pclm.0000152.

Kutz, S. J., E. P. Hoberg, L. Polley, and E. J. Jenkins. 2005. “Global Warming Is Changing the Dynamics of Arctic Host-Parasite Systems.” *Proceedings: Biological Sciences* 272 (1581): 2571–76.

Labaude, Sophie, Yannick Moret, Frank Cézilly, Charel Reuland, and Thierry Rigaud. 2017. “Variation in the Immune State of *Gammarus pulex* (Crustacea, Amphipoda) According to Temperature: Are Extreme Temperatures a Stress?” *Developmental & Comparative Immunology* 76 (November):25–33. https://doi.org/10.1016/j.dci.2017.05.013.

Laughton, Alice M., Cian O. O'Connor, and Robert J. Knell. 2017. "Responses to a Warming World: Integrating Life History, Immune Investment, and Pathogen Resistance in a Model Insect Species." *Ecology and Evolution* 7 (22): 9699–9710. https://doi.org/10.1002/ece3.3506.

Luković, Jelena, John C. H. Chiang, Dragan Blagojević, and Aleksandar Sekulić. 2021. "A Later Onset of the Rainy Season in California." *Geophysical Research Letters* 48 (4): e2020GL090350. https://doi.org/10.1029/2020GL090350.

Lyberger, Kelsey, Johannah Farner, Lisa Couper, and Erin A. Mordecai. 2024. "A Mosquito Parasite Is Locally Adapted to Its Host but Not Temperature." *The American Naturalist* 204 (2): 121–32. https://doi.org/10.1086/730522.

Martin, Lindsay E., and Julián F. Hillyer. 2024. "Higher Temperature Accelerates the Aging-Dependent Weakening of the Melanization Immune Response in Mosquitoes." *PLOS Pathogens* 20 (1): e1011935. https://doi.org/10.1371/journal.ppat.1011935.

Mazé-Guilmo, Elise, Simon Blanchet, Olivier Rey, Nicolas Canto, and Géraldine Loot. 2016. "Local Adaptation Drives Thermal Tolerance among Parasite Populations: A Common Garden Experiment." *Proceedings of the Royal Society B: Biological Sciences* 283 (1830): 20160587. https://doi.org/10.1098/rspb.2016.0587.

Mordecai, Erin A., Jamie M. Caldwell, Marissa K. Grossman, Catherine A. Lippi, Leah R. Johnson, Marco Neira, Jason R. Rohr, et al. 2019. "Thermal Biology of Mosquito-borne Disease." Edited by James (Jeb) Byers. *Ecology Letters*, July, ele.13335. https://doi.org/10.1111/ele.13335.

Mordecai, Erin A., Jeremy M. Cohen, Michelle V. Evans, Prithvi Gudapati, Leah R. Johnson, Catherine A. Lippi, Kerri Miazgowicz, et al. 2017. "Detecting the Impact of Temperature

535 on Transmission of Zika, Dengue, and Chikungunya Using Mechanistic Models." *PLOS*
536 *Neglected Tropical Diseases* 11 (4): e0005568.
537 https://doi.org/10.1371/journal.pntd.0005568.
538 Mordecai, Erin A., Krijn P. Paaijmans, Leah R. Johnson, Christian Balzer, Tal Ben-Horin, Emily
539 de Moor, Amy McNally, et al. 2013. "Optimal Temperature for Malaria Transmission Is
540 Dramatically Lower than Previously Predicted." *Ecology Letters* 16 (1): 22–30.
541 https://doi.org/10.1111/ele.12015.
542 Murdock, C. C., Krijn P. Paaijmans, Andrew S. Bell, Jonas G. King, Julián F. Hillyer, Andrew F.
543 Read, and Matthew B. Thomas. 2012. "Complex Effects of Temperature on Mosquito
544 Immune Function." *Proceedings of the Royal Society B: Biological Sciences* 279 (1741):
545 3357–66. https://doi.org/10.1098/rspb.2012.0638.
546 NOAA National Centers for Environmental Information. 2022. "Monthly National Climate
547 Report for 2022." https://www.ncei.noaa.gov/access/monitoring/monthly-
548 report/national/202408.
549 ———. 2023. "Monthly National Climate Report for 2023."
550 https://www.ncei.noaa.gov/access/monitoring/monthly-report/national/202408.
551 Padfield, Daniel, Meaghan Castledine, and Angus Buckling. 2020. "Temperature-Dependent
552 Changes to Host–Parasite Interactions Alter the Thermal Performance of a Bacterial
553 Host." *The ISME Journal* 14 (2): 389–98. https://doi.org/10.1038/s41396-019-0526-5.
554 Palmer-Young, Evan C., Lyna Ngor, Rodrigo Burciaga Nevarez, Jason A. Rothman, Thomas R.
555 Raffel, and Quinn S. McFrederick. 2019. "Temperature Dependence of Parasitic Infection
556 and Gut Bacterial Communities in Bumble Bees." *Environmental Microbiology* 21 (12):
557 4706–23. https://doi.org/10.1111/1462-2920.14805.

Paull, Sara H., Bryan E. LaFonte, and Pieter T. J. Johnson. 2012. "Temperature-Driven Shifts in a Host-Parasite Interaction Drive Nonlinear Changes in Disease Risk." *Global Change Biology* 18 (12): 3558–67. https://doi.org/10.1111/gcb.12018.

Penczykowski, Rachel M., Spencer R. Hall, David J. Civitello, and Meghan A. Duffy. 2014. "Habitat Structure and Ecological Drivers of Disease." *Limnology and Oceanography* 59 (2): 340–48. https://doi.org/10.4319/lo.2014.59.2.0340.

Petzoldt, Thomas. 2022. "R Package Growthrates."

Praskievicz, Sarah, and Heejun Chang. 2009. "Winter Precipitation Intensity and ENSO/PDO Variability in the Willamette Valley of Oregon." *International Journal of Climatology* 29 (13): 2033–39. https://doi.org/10.1002/joc.1838.

PRISM Climate Group, and Oregon State University. 2021. "PRISM Gridded Climate Data." https://prism.oregonstate.edu.

Ragonese, Isabella G., Maya R. Sarkar, Richard J. Hall, and Sonia Altizer. 2024. "Extreme Heat Reduces Host and Parasite Performance in a Butterfly–Parasite Interaction." *Proceedings of the Royal Society B: Biological Sciences* 291 (2015): 20232305. https://doi.org/10.1098/rspb.2023.2305.

Ryan, Sadie J., Colin J. Carlson, Erin A. Mordecai, and Leah R. Johnson. 2019. "Global Expansion and Redistribution of *Aedes*-Borne Virus Transmission Risk with Climate Change." *PLOS Neglected Tropical Diseases* 13 (3): e0007213. https://doi.org/10.1371/journal.pntd.0007213.

Seppälä, Otto, Katri Liljeroos, Anssi Karvonen, and Jukka Jokela. 2008. "Host Condition as a Constraint for Parasite Reproduction." *Oikos* 117 (5): 749–53. https://doi.org/10.1111/j.0030-1299.2008.16396.x.

Shah, Melisa M., Amy R. Krystosik, Bryson A. Ndenga, Francis M. Mutuku, Jamie M. Caldwell, Victoria Otuka, Philip K. Chebii, et al. 2019. "Malaria Smear Positivity among Kenyan Children Peaks at Intermediate Temperatures as Predicted by Ecological Models." *Parasites & Vectors* 12 (1): 288. https://doi.org/10.1186/s13071-019-3547-z.

Shocket, Marta S., Alexander T. Strauss, Jessica L. Hite, Maja Šljivar, David J. Civitello, Meghan A. Duffy, Carla E. Cáceres, and Spencer R. Hall. 2018. "Temperature Drives Epidemics in a Zooplankton-Fungus Disease System: A Trait-Driven Approach Points to Transmission via Host Foraging." *The American Naturalist* 191 (4): 435–51. https://doi.org/10.1086/696096.

Shocket, Marta S., Anna B. Verwillow, Mailo G. Numazu, Hani Slamani, Jeremy M. Cohen, Fadoua El Moustaid, Jason Rohr, Leah R. Johnson, and Erin A. Mordecai. 2020. "Transmission of West Nile and Five Other Temperate Mosquito-Borne Viruses Peaks at Temperatures between 23°C and 26°C." Edited by Eduardo Franco, Talía Malagón, and Alyssa Gehman. *eLife* 9 (September):e58511. https://doi.org/10.7554/eLife.58511.

Shocket, Marta S., Sadie J. Ryan, and Erin A. Mordecai. 2018. "Temperature Explains Broad Patterns of Ross River Virus Transmission." *eLife* 7 (August):e37762. https://doi.org/10.7554/eLife.37762.

Sinclair, Brent J., Caroline M. Williams, and John S. Terblanche. 2012. "Variation in Thermal Performance among Insect Populations." *Physiological and Biochemical Zoology* 85 (6): 594–606. https://doi.org/10.1086/665388.

Sternberg, Eleanore D., and Matthew B. Thomas. 2014. "Local Adaptation to Temperature and the Implications for Vector-Borne Diseases." *Trends in Parasitology* 30 (3): 115–22. https://doi.org/10.1016/j.pt.2013.12.010.

604 Sun, Syuan-Jyun, Marcin K. Dziuba, Riley N. Jaye, and Meghan A. Duffy. 2023. "Temperature
605 Modifies Trait-Mediated Infection Outcomes in a *Daphnia*–Fungal Parasite System."
606 *Philosophical Transactions of the Royal Society B: Biological Sciences* 378 (1873):
607 20220009. https://doi.org/10.1098/rstb.2022.0009.
608 Suwanchaichinda, Chansak, and Susan M. Paskewitz. 1998. "Effects of Larval Nutrition, Adult
609 Body Size, and Adult Temperature on the Ability of *Anopheles gambiae* (Diptera:
610 Culicidae) to Melanize Sephadex Beads." *Journal of Medical Entomology* 35 (2): 157–
611 61. https://doi.org/10.1093/jmedent/35.2.157.
612 Swain, Daniel L., Baird Langenbrunner, J. David Neelin, and Alex Hall. 2018. "Increasing
613 Precipitation Volatility in Twenty-First-Century California." *Nature Climate Change* 8
614 (5): 427–33. https://doi.org/10.1038/s41558-018-0140-y.
615 Taylor, Rachel A., Sadie J. Ryan, Catherine A. Lippi, David G. Hall, Hossein A. Narouei-
616 Khandan, Jason R. Rohr, and Leah R. Johnson. 2019. "Predicting the Fundamental
617 Thermal Niche of Crop Pests and Diseases in a Changing World: A Case Study on Citrus
618 Greening." Edited by Luke Flory. *Journal of Applied Ecology*, July, 1365-2664.13455.
619 https://doi.org/10.1111/1365-2664.13455.
620 Tesla, Blanka, Leah R. Demakovsky, Erin A. Mordecai, Sadie J. Ryan, Matthew H. Bonds,
621 Calistus N. Ngonghala, Melinda A. Brindley, and Courtney C. Murdock. 2018.
622 "Temperature Drives Zika Virus Transmission: Evidence from Empirical and
623 Mathematical Models." *Proceedings of the Royal Society B: Biological Sciences* 285
624 (1884): 20180795. https://doi.org/10.1098/rspb.2018.0795.

Thomas, Matthew B., and Simon Blanford. 2003. “Thermal Biology in Insect-Parasite Interactions.” *Trends in Ecology & Evolution* 18 (7): 344–50. https://doi.org/10.1016/S0169-5347(03)00069-7.

Urban, M. C., G. Bocedi, A. P. Hendry, J.-B. Mihoub, G. Pe’er, A. Singer, J. R. Bridle, et al. 2016. “Improving the Forecast for Biodiversity under Climate Change.” *Science* 353 (6304): aad8466. https://doi.org/10.1126/science.aad8466.

Venesky, Matthew D., Joseph DeMarchi, Cari Hickerson, and Carl D. Anthony. 2022. “Does the Thermal Mismatch Hypothesis Predict Disease Outcomes in Different Morphs of a Terrestrial Salamander?” *Journal of Experimental Zoology Part A: Ecological and Integrative Physiology*, 1–10. https://doi.org/10.1002/jez.2581.

Washburn, J., M. Gross, D. Mercer, and Anderson. 1988. “Predator-Induced Trophic Shift of a Free-Living Ciliate: Parasitism of Mosquito Larvae by Their Prey.” *Science* 240 (4856): 1193–95. https://doi.org/10.1126/science.3131877.

Washburn, Jan O., and John R. Anderson. 1986. “Distribution of *Lambornella clarki* (Ciliophora: Tetrahymenidae) and Other Mosquito Parasites in California Treeholes.” *Journal of Invertebrate Pathology* 48 (3): 296–309. https://doi.org/10.1016/0022-2011(86)90058-3.

Washburn, Jan O., John R. Anderson, and David R. Mercer. 1991. “Parasitism of Newly-Hatched *Aedes sierrensis* (Diptera: Culicidae) Larvae by *Lambornella clarki* (Ciliophora: Tetrahymenidae) Following Habitat Flooding.” *Journal of Invertebrate Pathology* 58 (1): 67–74. https://doi.org/10.1016/0022-2011(91)90163-K.

646 **Tables**

647

Predictor	Estimate	Standard error	Z-value	p-value
Mean annual temperature	-0.22	0.22	-1.01	3.13×10^{-1}
Mean annual temperature^2	-0.43	0.21	-2.01	$\mathbf{4.45 \times 10^{-2}}$
Survey year	1.31	0.34	3.90	$\mathbf{9.5 \times 10^{-5}}$
*Mean annual temperature * survey year*	-0.45	0.26	-1.72	8.5×10^{-2}
Mean annual temperature^2 ** survey year*	-0.127	0.247	-0.52	6.34×10^{-1}

648

649 **Table 1. Results of a generalized linear mixed-effects model with tree hole infection status**
650 **as the dependent variable and mean annual temperature, mean annual temperature^2, and**
651 **survey year as fixed effects, and tree hole ID as a random effect.** P-values < 0.05 are
652 displayed in bold to highlight statistical significance.

653

654 **Figure captions**

655 **Figure 1. Tree holes were surveyed, and experimental host and parasite populations reared,**
656 **from across a large geographic temperature gradient on the western coast of the United**
657 **States during the 2022 (left) and 2023 (right) rainy seasons.** The mapped color gradient shows
658 mean temperature during the rainy season in Washington, Oregon, and California, USA, from the
659 4 km PRISM climate dataset. Points show the locations of 507 total surveyed tree holes. *L. clarki*
660 infection presence is indicated by black points, and absence by white points. Colored ovals
661 indicate the source locations of the six host populations used in the infection experiment (from
662 north to south: EUG = Eugene, OR; JR = Woodside, CA; FRS = Shaver Lake, CA; BIG = Big
663 Sur, CA; WHIT = Trabuco Canyon, CA; CAS = San Juan Capistrano, CA); the gray oval shows
664 the host population used in the melanization response experiment (PAR = Paso Robles, CA); and
665 the gray rectangle shows the source location of the ciliate parasite culture used in the infection
666 experiment (Marin = Novato, CA). Green outlines indicate tree holes in which iButtons logged
667 temperature data during the year between the two sampling visits.

668 **Figure 2. Infection probability followed a consistent hump-shaped relationship with mean**
669 **temperature during the rainy season, and was higher overall in 2023 compared to 2022. (A)**
670 Counts of infected (black) and uninfected (gray) tree holes across the climate gradient in each
671 survey year. **(B)** Generalized linear mixed-effects model predictions of infection probability by
672 temperature and year are plotted across the surveyed climate gradient for each year of the field
673 survey. The solid and dashed lines show the mean model predictions for 2022 and 2023,
674 respectively, and the shading shows the 95% confidence intervals.

675 **Figure 3. Thermal responses of host – parasite interaction outcomes were similar among**
676 **host populations from warm, intermediate, and cold source climates.** For each outcome

measured in the infection experiment, mean estimated TPCs for each of six host populations are shown (lines) with 95% credible intervals (shading). The left column shows initial infection and parasite melanization responses up to the third experiment checkpoint, when the first deaths of infected larvae released additional parasites into the environment. The right column shows the total infection, parasite melanization, and parasite-induced mortality rates across temperatures at the end of the experiment. Mortality rates were significantly higher near 10 ºC for population BIG compared to populations JR and EUG. The TPCs shown here are presented individually, with the experiment data, in Appendix S2 (Figures S2, S4, S6, S8, S10).

Figure 4. Experimental infections were most likely to occur at cold incubation temperatures where the host melanization response and development were suppressed. (A) Points show mean values, error bars show +/- 1 SE, lines show mean estimated TPCs, and shading shows 95% credible intervals for key host – parasitism interaction outcomes and processes: free-living parasite population growth (green); the host mechanically stimulated melanization immune response (black); the initial infection rate (light pink), calculated up to the first fatality at each temperature; the total infection rate (dark pink); and total mortality (gray) calculated up to the first pupation at each temperature. The infection data shown include all host populations in the infection experiment. **(B)** Infection (top; dark pink), parasite-induced mortality (middle; light gray), and parasite melanization (bottom; dark gray) counts are plotted over time for each temperature used in the infection experiment. Colored points show data from individual microcosms, and black points and lines show mean trajectories +/- 1 SE. For each temperature, the final experiment checkpoint was at the time of the first observed pupation.

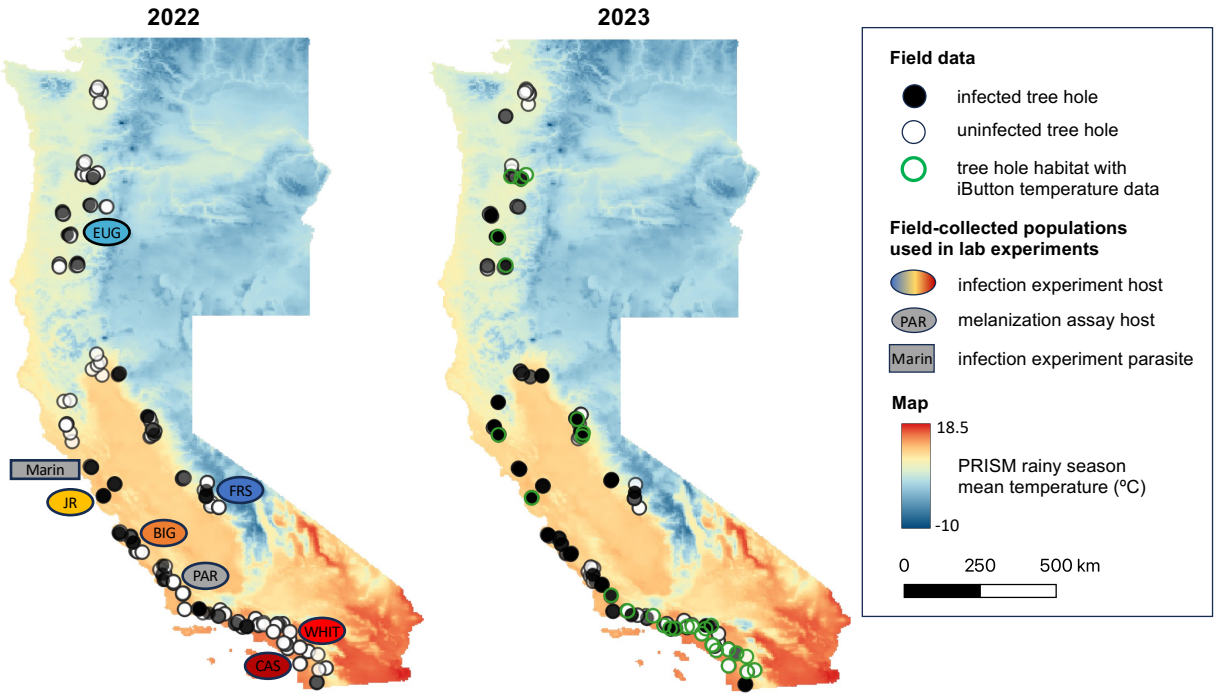

698

699 **Figure 1.**

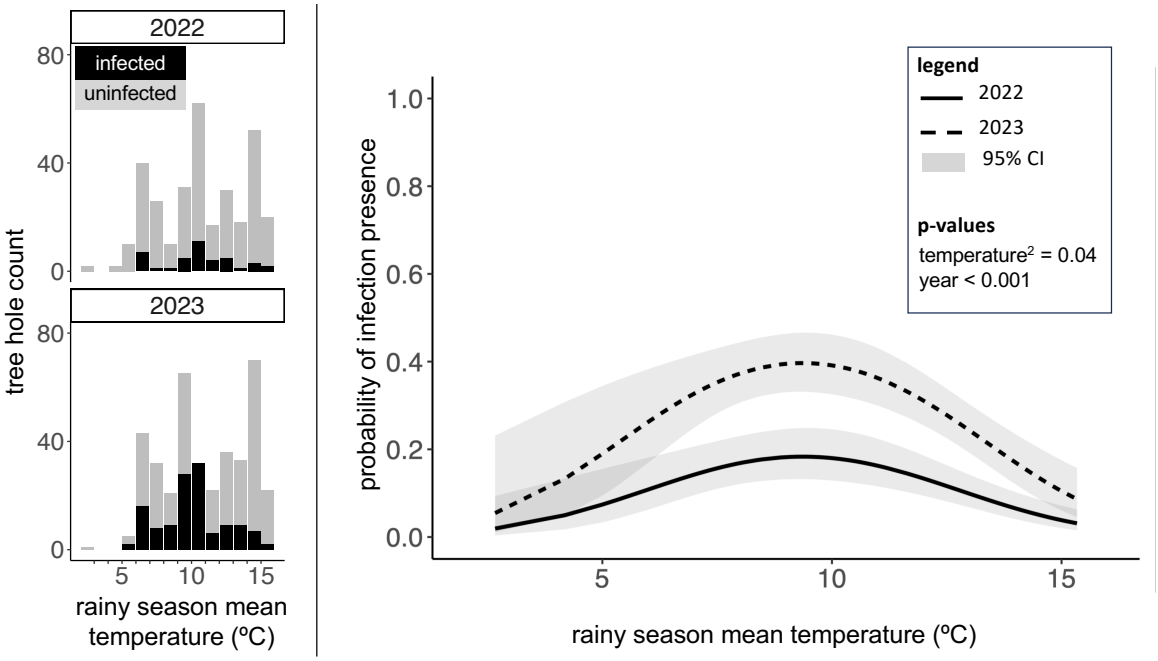
2022
infected
uninfected
2023
tree hole count
80
40
0
5
10
15
rainy season mean temperature (ºC)
probability of infection presence
1.0
0.8
0.6
0.4
0.2
0.0
legend
2022
2023
95% CI
p-values
temperature² = 0.04
year < 0.001
rainy season mean temperature (ºC)

Figure 2.

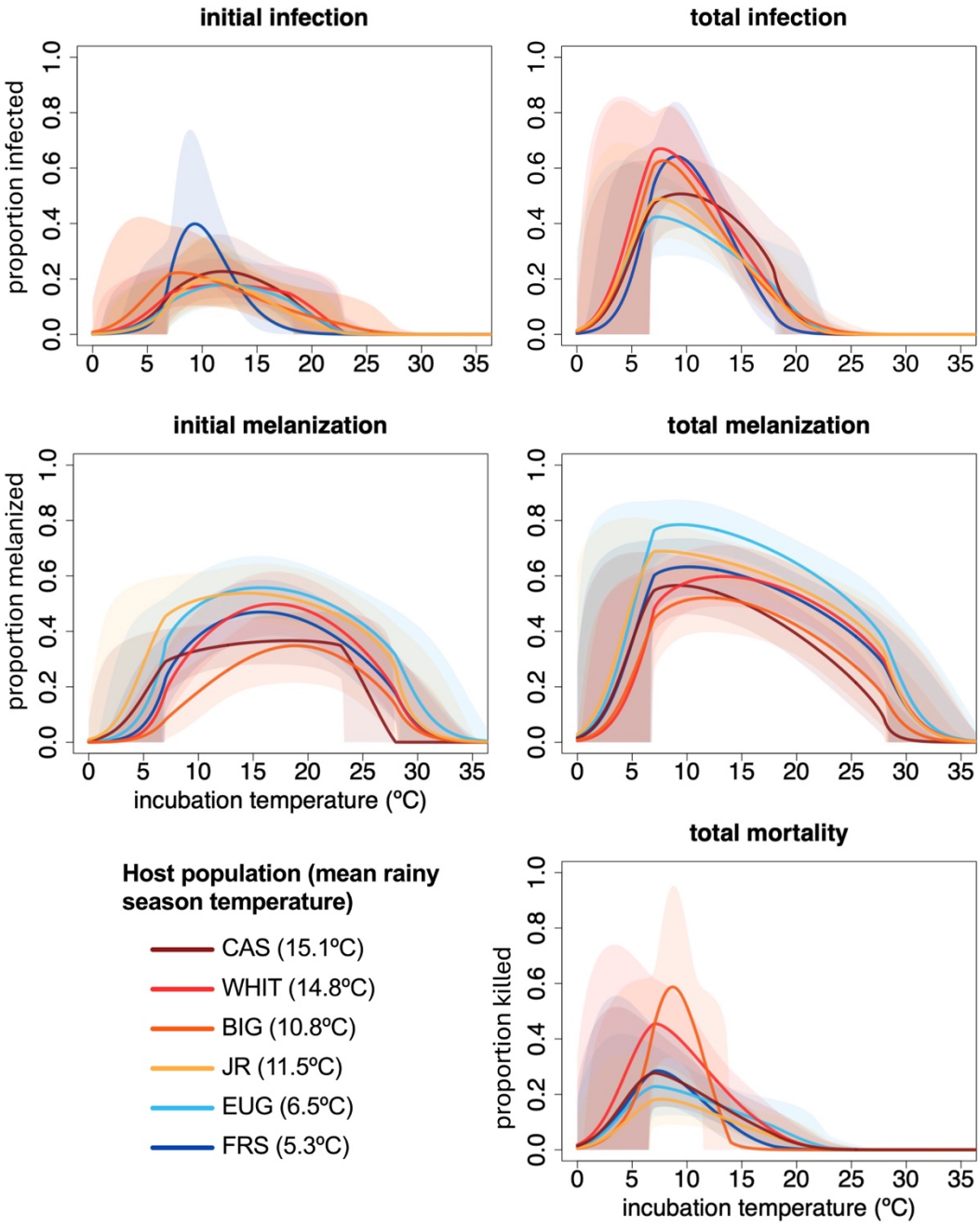
initial infection
total infection
initial melanization
total melanization
total mortality
proportion infected
proportion melanized
proportion killed
incubation temperature (°C)
Host population (mean rainy season temperature)
CAS (15.1°C)
WHIT (14.8°C)
BIG (10.8°C)
JR (11.5°C)
EUG (6.5°C)
FRS (5.3°C)

Figure 3.

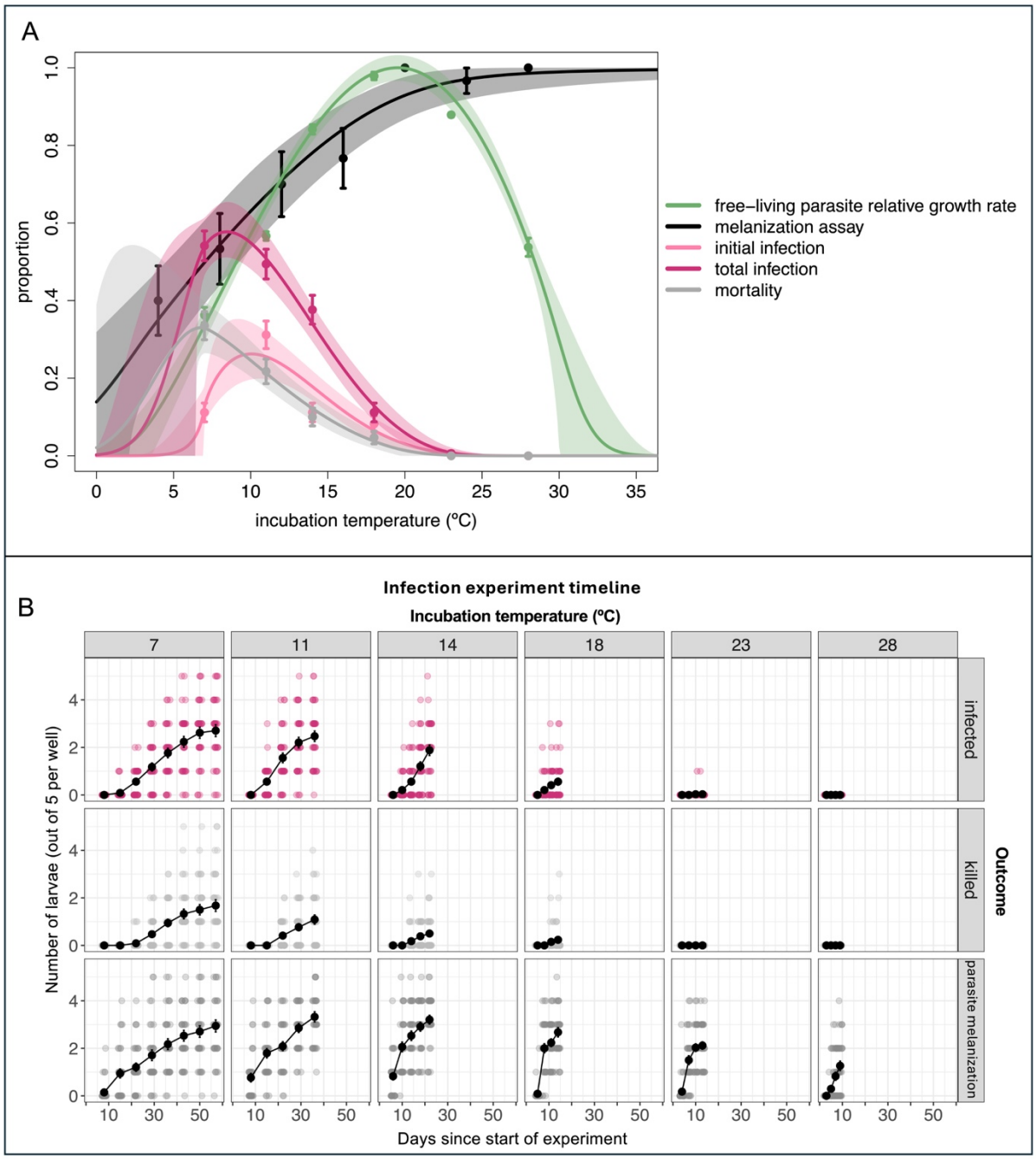
A
proportion
0.0
0.2
0.4
0.6
0.8
1.0
0
5
10
15
20
25
30
35
incubation temperature (°C)
free−living parasite relative growth rate
melanization assay
initial infection
total infection
mortality
B
Infection experiment timeline
Incubation temperature (°C)
7
11
14
18
23
28
infected
killed
parasite melanization
Outcome
Number of larvae (out of 5 per well)
0
2
4
10
30
50
Days since start of experiment

Figure 4.